J. Magn. Soc. Jpn., **41**, 20-24 (2017)

<Paper>

Synthesis and magnetic properties of Fe substituted hibonite

H. Nagumo*, K. Watanabe**, K. Kakizaki*, and K. Kamishima*

* Graduate School of Science and Engineering, Saitama University, *255 Shimo-Okubo, Saitama 338—0825, Japan*

** Biomolecular Characterization Unit, Center for Sustainable Resource Science, RIKEN, *2-1 Wako, Saitama 351—0198, Japan*

We have investigated the synthesis conditions and magnetic properties of Fe substituted hibonite with initial compositions of $CaAl_{12-x}Fe_xO_{19}$ ($0 \leq x \leq 12$) and $CaAl_{10-x}Fe_xO_{19-\delta}$ ($0 \leq x \leq 10$). The Fe doped hibonite can be synthesized at a sintering temperature of 1300˚C. The X–ray diffraction patterns of Fe substituted hibonite samples are in good agreement with the pattern of hibonite. The lattice parameter increased due to the difference between the radius of Al^{3+} and that of Fe^{3+}. The magnetization and Curie temperature of the best sample ($CaAl_2Fe_8O_{19-\delta}$) are 31 emu/g and 290˚C, respectively.

Keywords: M–type, hexaferrite

1. Introduction

M-type ferrites (Ba, Sr, Pb)$Fe_{12}O_{19}$ have high magnetization and coercivity, which leads to application as a permanent magnet. Consequently, M-type ferrites have long been the subject of intensive research.[1)]

Ca-based M–type ferrite is an attractive subject because of the rich resource of its Fe and Ca elements. Fe and Ca are widespread elements in minerals, as implied by the 4th and 5th largest Clarke numbers of Fe and Ca.[2)] However, there is no $CaFe_{12}O_{19}$ phase in the CaO-Fe_2O_3 diagram.[3), 4)] This Ca-based M-type ferrite can be stabilized only by the addition of a rare-earth element of La.[5)–7)]

The crystal structure of M-type ferrite is similar to that of hibonite ($CaAl_{12}O_{19}$) except that the structure models are divided on the interpretation of the bipyramidal Al^{3+} ions.[8)] Figure 1 shows the crystal structure of $CaAl_{12}O_{19}$ along [010] view direction. The unit cell contains two chemical formulas of $CaAl_{12}O_{19}$ like M-type ferrite. To the best of our knowledge, the systematic substitution effect of Fe^{3+} for Al^{3+} of $CaAl_{12}O_{19}$ has not been reported yet in spite of the similarity in the crystal structures.[9)]

In this study, we have investigated the synthesis conditions and magnetic properties of the Fe substituted hibonite.

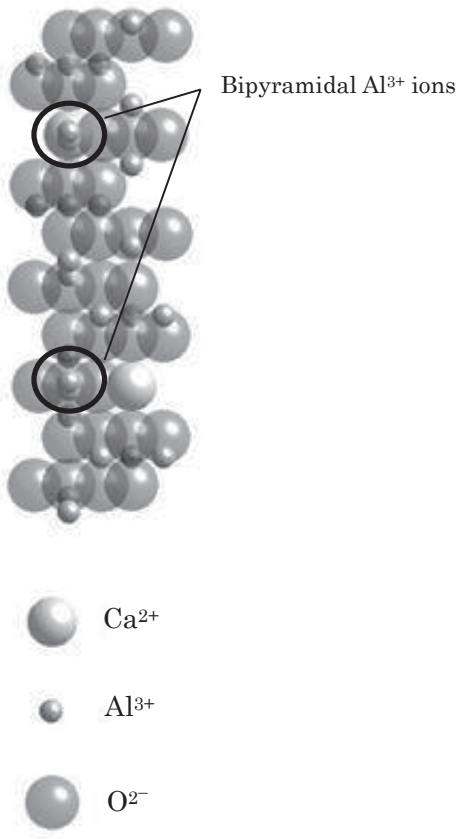

Fig. 1 Crystal structure of hibonite along [010] view direction.

2. Experimental procedure

Samples were prepared by a conventional ceramic method. We used $CaCO_3$, Al_2O_3, and α–Fe_2O_3 as starting materials. Before we mixed them, we heated Al_2O_3 powder at 500˚C for an hour in order to remove water molecules on the material. They were mixed in the desired proportions of $CaAl_{12-x}Fe_xO_{19}$ ($0 \leq x \leq 12$) and $CaAl_{10-x}Fe_xO_{19-\delta}$ ($0 \leq x \leq 10$) in a ball-milling pot for 24 h. The mixed powder was pressed into a disk shape. The disk was pre-sintered in air at 900˚C for 5 h. The sintered sample was pounded in a mortar and then ground into fine powder using a planetary ball mill for 10 minutes at 1100 rpm (Fritsch, P–7 Premium line). The powder was pressed into a disk shape. The disks were heated at 1100—1400˚C for 5 h. X-ray diffraction (XRD) analysis with Cu-Kα radiation was performed to characterize the crystalline samples. The magnetic properties were measured by using a vibrating sample magnetometer (Tamakawa TM-VSM2130HGC). The chemical composition was examined by using a commercial electron probe micro analyzer (EPMA) (JEOL, JXA – 8200).

3. Results and discussion

Figure 2 shows the X–ray diffraction patterns of the sintered samples at 1300˚C whose starting powder was mixed at the iron-substituted-hibonite chemical composition of Ca: Al: Fe=1:(12–x):x. The hibonite chemical composition sample (x=0) exhibits the mixed phases of Al_2O_3, $CaAl_4O_7$, and $CaAl_2O_4$. The hibonite phase was formed by the substitution of Fe for Al at x≥1. The diffraction peaks of the hibonite phase shifted to the low angle side with increasing the Fe content.

The (Al+Fe)/Ca ratio of twelve to one may be too large for the reaction to form the hibonite phase because the starting material of α–Fe_2O_3 remained at x≥7 (iron rich compositions). In the same way, that of Al_2O_3 did not react at x≤2 (aluminum rich compositions).

Figure 3 shows the lattice constants of the hibonite phase in the $CaAl_{12-x}Fe_xO_{19}$ (0≤x≤12) initial composition samples sintered at 1300˚C. The lattice constants a and c were obtained using Cohen's least square method.[10] a and c gradually increased with the amount of Fe^{3+} ions

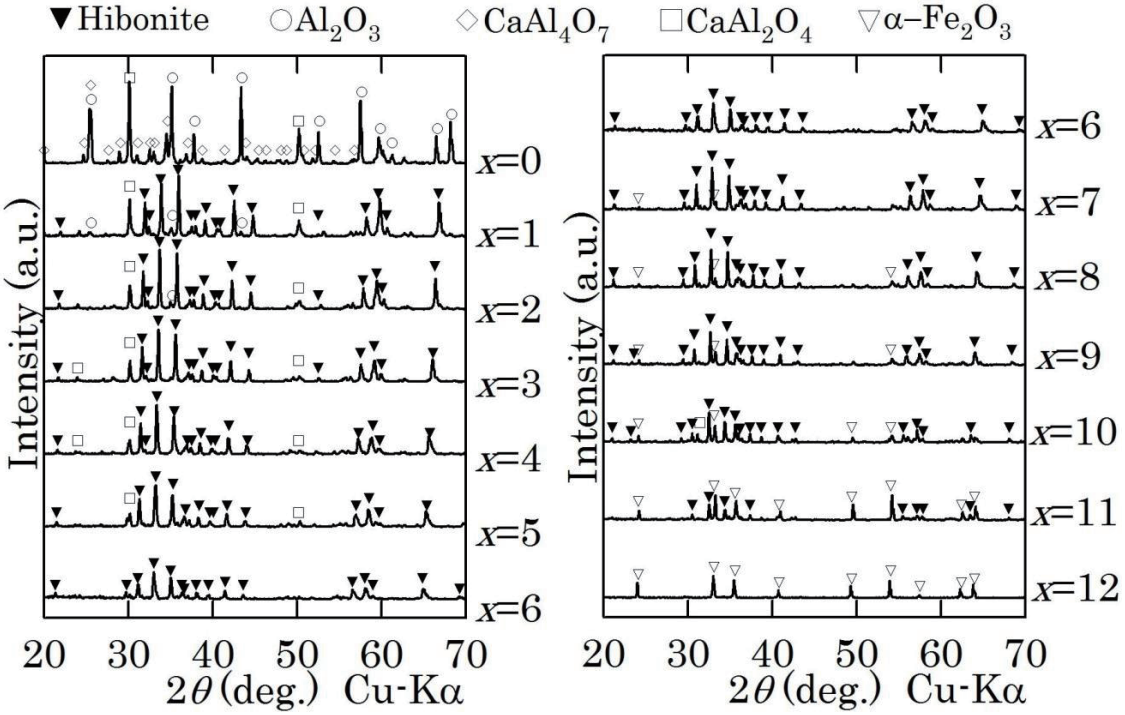

Fig. 2 X-ray diffraction patterns of the $CaAl_{12-x}Fe_xO_{19}$ (0≤x≤12) initial composition samples sintered at 1300˚C.

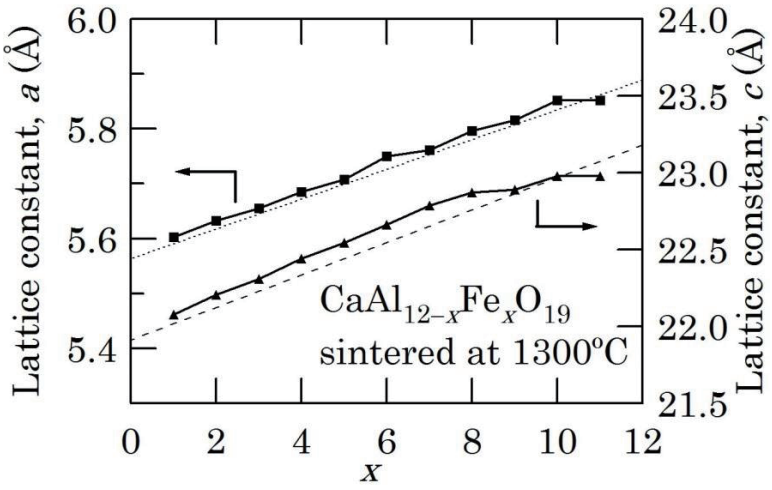

Fig. 3 Lattice constants of the $CaAl_{12-x}Fe_xO_{19}$ (1≤x≤11) initial composition samples sintered at 1300˚C.

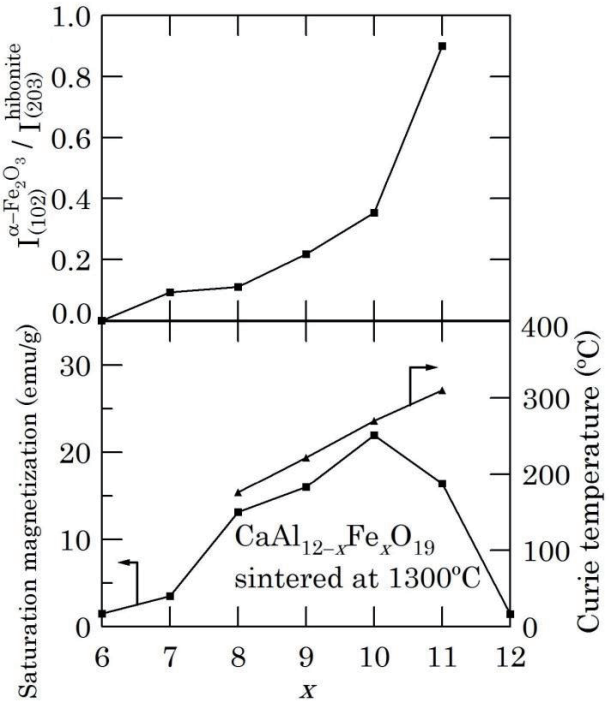

Fig. 4 Saturation magnetization and Curie temperature of the $CaAl_{12-x}Fe_xO_{19}$ ($6 \leq x \leq 12$) initial composition samples sintered at 1300˚C. The intensity ratio of the α–Fe_2O_3 (102) plane to the hibonite (203) plane is also shown.

because the ionic radius of an Fe^{3+} ion r[Fe^{3+}] is larger than that of an Al^{3+} ion r[Al^{3+}]; r[Fe^{3+}, HS]=0.49 Å > r[Al^{3+}]=0.39 Å at a tetrahedral site and r[Fe^{3+}, HS]=0.645 Å > r[Al^{3+}]=0.535 Å at an octahedral site, where "HS" denotes the high spin configuration of electrons. [11] The dotted straight lines are connected between the lattice constants of the hibonite (x=0) and the typical M-type ferrite ($SrFe_{12}O_{19}$) in which the ionic radius of Sr is similar to that of Ca. Our results are close to these dotted lines, which implies that a linear relation exists between the lattice constant and the concentrations of the constituent elements (Vegard's law).[12]

Figure 4 shows the saturation magnetization (M_S) at room temperature, the Curie temperature (T_C), and the relative intensity $I^{\alpha-Fe_2O_3}_{(102)}/I^{hibonite}_{(203)}$ of the Fe rich composition samples ($CaAl_{12-x}Fe_xO_{19}$; $x \geq 6$). The samples at x<7 had small magnetizations at room temperature in spite of the single crystallographic phase of hibonite. This fact reflects the small intrinsic magnetic moment and low T_C due to the small amount of the iron cations. With increasing the iron content up to x=10, M_S increased although the relative intensity of α–Fe_2O_3 gradually increased. This increase of M_S is due to the replacement of non-magnetic Al^{3+} to magnetic Fe^{3+} ions of magnetic hibonite phase in these samples. On the other hand, M_S decreased with increasing the iron content above x=10. This is consistent with the fact that the diffraction peaks of hibonite became weak and finally disappeared at x=12.

The Curie temperature was increased by iron substitution. Because nonmagnetic Al^{3+} ions were

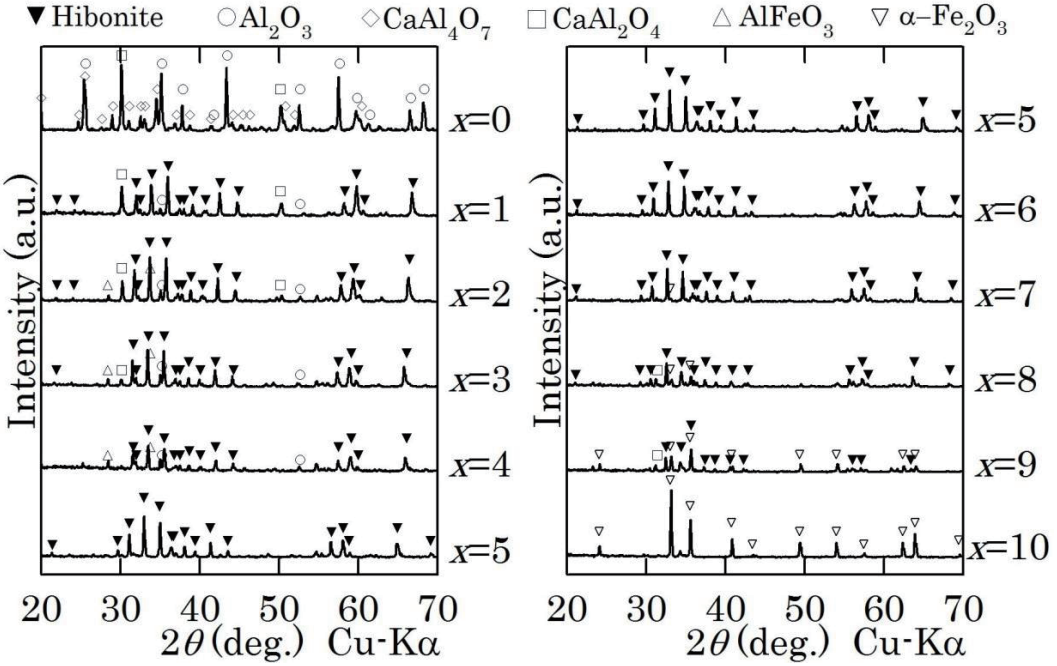

Fig. 5 X-ray diffraction patterns of the $CaAl_{10-x}Fe_xO_{19-\delta}$ ($0 \leq x \leq 10$) initial composition samples sintered at 1300˚C.

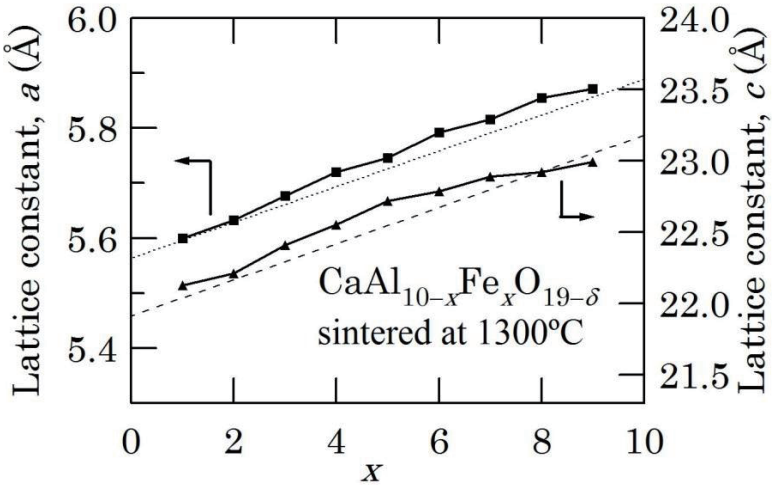

Fig. 6 Lattice constant of the $CaAl_{10-x}Fe_xO_{19-\delta}$ ($1 \leq x \leq 9$) initial composition samples sintered at 1300˚C.

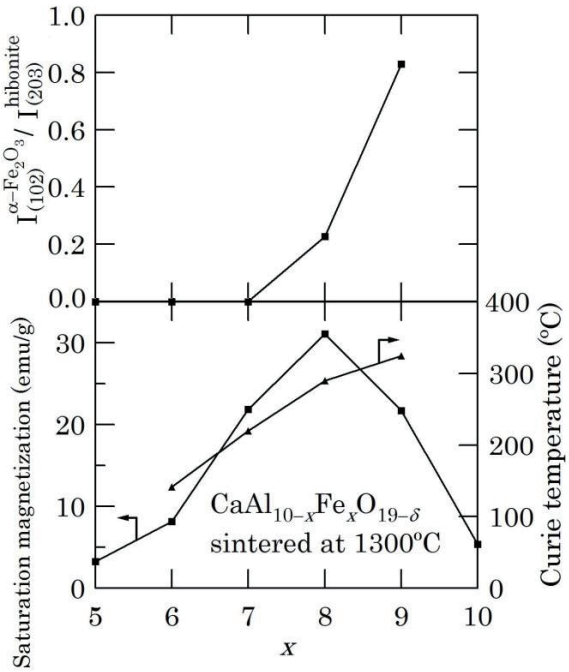

Fig. 7 Saturation magnetization and Curie temperature of the $CaAl_{10-x}Fe_xO_{19-\delta}$ ($5 \leq x \leq 10$) initial composition samples sintered at 1300˚C. The intensity ratio of the α–Fe_2O_3 (102) plane to the hibonite (203) plane is also shown.

Table 1 Chemical composition of the x=8 sample ($CaAl_2Fe_8O_{19-\delta}$) sintered at 1300˚C.

	Ca→1	Initial
Ca	1	1
Al	1.75	2
Fe	7.11	8

replaced by magnetic Fe^{3+} ions, the average superexchange interaction between magnetic Fe^{3+} ions in the sample can operate. The increase of the amount of the iron cations and their interactions may lead to the rise of T_C. T_C was increased up to x=11 even though M_S was decreased from x=10 to x=11. This means that the magnetic hibonite phase was formed with excessive α–Fe_2O_3 at x=11. The excess of α–Fe_2O_3 at x=11 is also implied by the abrupt increase of $I_{(102)}^{\alpha\text{-}Fe_2O_3}/I_{(203)}^{hibonite}$ from x=10 to x=11 in Fig. 4. This result also suggests that the (Al+Fe)/Ca ratio of twelve to one is too large for the formation of the hibonite phase. This is consistent with the XRD result shown in Fig. 2.

These experimental results of $CaAl_{12-x}Fe_xO_{19}$ led us to the next experiments to decrease the (Al+Fe)/Ca ratio in iron-substituted hibonite. We changed the starting composition from $CaAl_{12-x}Fe_xO_{19}$ to $CaAl_{10-x}Fe_xO_{19-\delta}$ in order to prevent the excess of α–Fe_2O_3 and to improve the magnetic properties.

Figure 5 shows the X-ray diffraction patterns of the sintered samples at 1300˚C whose starting powder was mixed at the chemical composition of Ca:Al:Fe=1:(10–x):x. After we changed the starting composition from $CaAl_{12-x}Fe_xO_{19}$ to $CaAl_{10-x}Fe_xO_{19-\delta}$, peaks of hematite became weaker at the iron rich compositions.

Figure 6 shows the lattice constants of the $CaAl_{10-x}Fe_xO_{19-\delta}$ ($0 \leq x \leq 10$) initial composition samples sintered at 1300˚C. The dotted straight lines are connected between the lattice constants of the hibonite (x=0) and $SrFe_{12}O_{19}$. The substitution–dependent variation of lattice constants ($\Delta a/\Delta x$ and $\Delta c/\Delta x$) of $CaAl_{10-x}Fe_xO_{19-\delta}$ at the Fe rich compositions is larger than that of $CaAl_{12-x}Fe_xO_{19}$ ($x \geq 10$). In addition, the X-ray diffraction peaks of the remaining α–Fe_2O_3 in $CaAl_{10-x}Fe_xO_{19-\delta}$ are weaker than those in $CaAl_{12-x}Fe_xO_{19}$ at the Fe rich compositions. These facts indicate that the substitution of Fe^{3+} for Al^{3+} in $CaAl_{10-x}Fe_xO_{19-\delta}$ is

more successful than in $CaAl_{12-x}Fe_xO_{19}$.

Figure 7 shows the saturation magnetization (M_S) at room temperature and the Curie temperature (T_C) and the relative intensity $I_{(102)}^{\alpha-Fe_2O_3}/I_{(203)}^{hibonite}$ of the Fe rich composition samples. The iron-substitution dependence is similar to that of $CaAl_{12-x}Fe_xO_{19}$ in Fig. 4. However, the value of M_S was higher than that of $CaAl_{12-x}Fe_xO_{19}$ composition samples. The maximum T_C was 325°C for $CaAl_{10-x}Fe_xO_{19-\delta}$ at x=9. It should be noted that this maximum Curie temperature is higher than the maximum T_C of $CaAl_{12-x}Fe_xO_{19}$ at x=11. The relative intensity $I_{(102)}^{\alpha-Fe_2O_3}/I_{(203)}^{hibonite}$ is also lower than that in Fig. 4. These facts suggest that the starting material composition of Ca: Al: Fe=1:(10–x):x is more suitable for the synthesis of iron-substituted magnetic hibonite.

Table 1 shows the estimated chemical composition of the x=8 sample ($CaAl_2Fe_8O_{19-\delta}$) sintered at 1300°C. By the use of EPMA, we measured the compositions of 50 particles of this sample. The table shows the average composition. The elements of Ca, Al, and Fe were in the ratio 1: 1.75: 7.11. The ratio of Ca is slightly higher than the initial ratio of 1: 2: 8. This may be caused by the elution of the Ca-rich oxide (e.g., $CaFe_2O_4$ with melting point of 1216°C) on the sample grains.[3)]

4. Conclusion

Fe^{3+} substituted hibonite–phase samples have been successfully synthesized by a conventional ceramic method with the modified initial chemical compositions of $CaAl_{10-x}Fe_xO_{19-\delta}$. XRD patterns of $CaAl_{10-x}Fe_xO_{19-\delta}$ sintered at 1300°C demonstrated the hibonite phase at $1 \leq x \leq 9$. The lattice parameter increased with increasing Fe^{3+} content. The maximum saturation magnetization was 31 emu/g at x=8 ($CaAl_2Fe_8O_{19-\delta}$). The Curie temperature rose up to 325°C with the replacement of Al^{3+} ions by Fe^{3+} ions.

References

1) J. Smit and H. P. J. Wijn: Ferrites, 177—211 (Philips Technical Library, 1959).
2) F. W. Clark and H. S. Washington: The Composition of the Earth's Crust, 34 (Government Printing Office, 1924).
3) B. Phillips and A. Muan: *J. Am. Ceram.* Soc., **41**, 445—454 (1958).
4) B. S. Boyanov: *J. Min. Met.* , **41 B**, 67—77 (2005).
5) N. Ichinose and K. Kurihara: *J. Phys. Soc. Jpn.*, **18**, 1700—1701 (1963).
6) H. Yamamoto, T. Kawaguchi, and M. Nagakura: *IEEE Trans. Magn.*, **15**, 1141—1146 (1979).
7) Y. Kobayashi, S, Hosokawa, E. Oda, and S. Toyota: *J. Jpn. Soc. Powder Powder Metall.*, **v. 55-7**, 541—546 (2008).
8) A. Utsunomiya, K. Tanaka, H. Morikawa, F. Marumo, and H. Kojima: *J. Solid State Chem.*, **75**, 197—200 (1988).
9) J. B. MacChesney, R.C. Sherwood, E. T. Keve, P. B. O'Connor, and L. D. Blitzer: Proc. Int. Conf. Ferrites, Kyoto, 1970, 158 (1971).
10) B. D. Cullity: Elements of X-ray Diffraction, 342 (Addison-Wesley, 1967).
11) R. D. Shannon, *Acta Cryst.* **A 32**, 751-767 (1976).
12) L. Vegard, *Z. Physik*, **5**, 17 (1921).

Received Jul. 30, 2016; Revised Oct. 3, 2016; Accepted Dec. 9, 2016